Received: 15 May 2023 | Revised: 18 October 2023 | Accepted: 25 October 2023

DOI: 10.1111/jace.19540

Journal of the American Ceramic Society

SPECIAL ISSUE ARTICLE

Examining the ferroelectric characteristics of aluminum nitride-based thin films

Binghui Deng | **Yanming Zhang** | **Yunfeng Shi**

Department of Materials Science and Engineering, Rensselaer Polytechnic Institute, Troy, New York, USA

Correspondence
Binghui Deng and Yunfeng Shi, Department of Materials Science and Engineering, Rensselaer Polytechnic Institute, Troy, NY 12180, USA.
Email: dengb4@rpi.edu and shiy2@rpi.edu

Abstract

The discovery of ferroelectricity in AlN-based thin films, including $Al_{1-x}Sc_xN$ and $Al_{1-x}B_xN$, over the past few years has spurred great research interests worldwide. In this review, we carefully examined the latest developments for these ferroelectric films with respect to alloy composition, temperature, film thickness, deposition condition, and fatigue endurance by electric field cycling. Looking ahead, there is an urgent need to resolve the challenge of large current leakage faced by these films, which necessitates a combined efforts from both simulations and experiments to identify the root cause and eventually come up with engineering strategies to suppress such leakage. In addition, overcoming the thickness scaling challenge to push ferroelectric thin film down to a few nanometers for better device miniaturization will also be of great interest. Considering the somewhat unexpected discovery of AlN-based thin films with potential ferroelectric application, we believe that it will be also rewarding to further explore other III-V-based semiconductor materials.

KEYWORDS
aluminum nitride, ferroelectricity, polarization, thin films

1 | INTRODUCTION

Ferroelectric materials, exhibiting two polarization states and are capable of being switched back and forth with an external electric field, are playing significant roles in the semiconductor industry.[1–3] They are mainly characterized by the remanent polarization P_r, in the absence of electric field, and coercive field E_c at which polarization can be switched. Ferroelectricity requires a crystal to be structurally polar noncentrosymmetric in such a way that the position of one or several ions in the unit cell is capable of switching between two states under external electric field without jeopardizing the stability of the crystal.[4] For this reason, ferroelectricity is historically limited among generally complex oxides involving multiple elements, such as $BaTiO_3$,[5–7] $Pb(Zr,Ti)O_3$,[8–10] $SrBi_2Ta_2O_9$,[11–13] and $BiFeO_3$[14–16] perovskite materials. However, commercial applications of the above materials in semiconductor industry have been limited due to challenges in meeting the demanding requirements for thermal budget, control of production-line-compatible elements, and exposure to forming gas anneal.[4] In 2011, ferroelectricity was first demonstrated in silicon-doped hafnium oxide (HfO_2)[17] thin film, which has fueled new research interests and promises for integrating ferroelectrics into metal-oxide-semiconductor fabrication process.[18–24]

More recently, another significant development of ferroelectrics is the realization of ferroelectricity in scandium-substituted AlN thin films by Fichtner et al.[25] in 2019 and boron-substituted AlN thin films by Hayden et al.[26] in 2021. The aforementioned discovery is motivated by a quantum mechanical calculation showing that the addition of scandium into III-nitride, such as AlN, significantly flattens the energy landscape so that polarization

switching is facilitated.[27] Different from conventional perovskite ferroelectric materials with performance adversely affected by the presence of extensive oxygen vacancies, nitride ferroelectrics have relatively less nitrogen vacancies because of stronger metal-nitride bond and higher vacancy formation energy,[28] thus promising better endurance performance.[4,29,30] In addition, it has been demonstrated that these novel ferroelectric films exhibit large P_r,[25,26] tunable E_c,[31–33] and high temperature stability.[34,35] With characteristics of ferroelectric, pyroelectric, and piezoelectric all together, these materials therefore have a wide range of potential applications, such as capacitors, memories, actuators, and sensors.[1] To date, although there have been a few great comprehensive reviews on ferroelectric materials and devices,[2,4,30] it is the aim of this work to dedicatedly examine the latest developments of AlN-based ferroelectric thin films, including pure AlN, $Al_{1-x}Sc_xN$, and $Al_{1-x}B_xN$ thin films. For topics not covered in this work, it is highly recommended to check them out in those reviews.

2 | FERROELECTRICITY IN AlN THIN FILM

The spontaneous polarization in wurtzite AlN has been well known for a long time, but ferroelectric switching has never been realized due to dielectric breakdown prior to reaching E_c. In 2019, Lin et al.[36] first reported ferroelectricity in pure AlN ultrathin films prepared by atomic layer epitaxy. The fundamental rationale underlying this work is based on the hypothesis that E_c could be significantly lowered by strain engineering in AlN films. Specifically, they grew the AlN thin films epitaxially on the GaN substrate by atomic layer deposition at 300°C to form a [0001]-oriented AlN/GaN epitaxial heterostructure. Due to the lattice mismatch, in-plane tensile stress is expected to be present in the AlN thin films.

Figure 1A,B shows the polarization hysteresis loops for the AlN thin films with thickness of 8, 10, 25, and 38 nm. Interestingly, soft ferroelectric characteristics are observed as shown by the sharp polarization switching in the 8- and 10-nm films. However, the polarization hysteresis loops in the 25- and 38-nm thick samples are quite different. The absence of ferroelectric hysteresis loops for the two thicker films could be explained by the gradual decay of strain away from the AlN/GaN interface to the point where strain is insufficient to lower E_c anymore, as shown in Figure 1C,D. Nevertheless, we want to draw attention that that P_r herein is nearly two orders of magnitude lower than theoretical prediction (~130 uC/cm^2)[25,37] even for the 8- and 10-nm-thick thin films, which calls for further investigation and validation of the results.

In addition, Yasuoka et al.,[32] Hayden et al.,[26] and Zhu et al.[38] all have explored the ferroelectric switching capability of pure AlN films fabricated by sputtering method. However, no complete polarization hysteresis loops could be demonstrated in Figure 2, even though limited partial polarization switching is present in these films. The exhibition of unambiguous ferroelectric characteristics for AlN thin film requires additional assistance from either tensile strain, temperature, or film fabrication quality to lower the coercive field.

3 | FERROELECTRICITY IN $Al_{1-x}SC_xN$ THIN FILM

3.1 | Experimental demonstration and confirmation

In 2019, Fichtner et al.[25] first unambiguously demonstrated ferroelectric switching in $Al_{1-x}Sc_xN$ thin films as shown in Figure 3A. The polycrystalline films were prepared by reactive sputter deposition on a platinized Si wafer substrate at 400°C. The final film thickness is 400 nm (x = 0.27), 600 nm (x = 0.32, 0.36, 0.40), and 1 μm (x = 0.43). Ferroelectricity is not observed for samples with $x < 0.27$ due to dielectric breakdown. Interestingly, both P_r and E_c decrease with increasing Sc content, which could be related to the continuous distortion of the original wurtzite-type crystal structure toward a layered-hexagonal structure as sketched in Figure 3B.[4] Specifically, the wurtzite basal plane as well as the internal parameter u (ratio of the metal-nitrogen bond length parallel to the c-axis relative to the lattice parameter c) increase, particularly at the Sc sites, with Sc being continuously doped into the film. The nonpolar hexagonal structure therefore could be seen as a transition state (u = 0.5) between the two polarization wurtzite structures to facilitate switching. In other words, the introduction of Sc flattens the ionic potential well toward the hexagonal structure and significantly lowers the energy barrier for ferroelectric switching.[27,39,40]

Yasuoka et al.[32] later confirmed the ferroelectricity in $Al_{1-x}Sc_xN$ films with x = 0.1–0.34, further extended the lower limit for Sc content from 0.27 to 0.1. Similarly, the films were prepared on a platinized Si substrate using reactive magnetron sputtering method at the deposition temperature of 400°C with the final film thickness of ~140 nm. The success for pushing ferroelectricity down to lower Sc content might be attributed to the fact that they successfully fabricated good quality films with higher

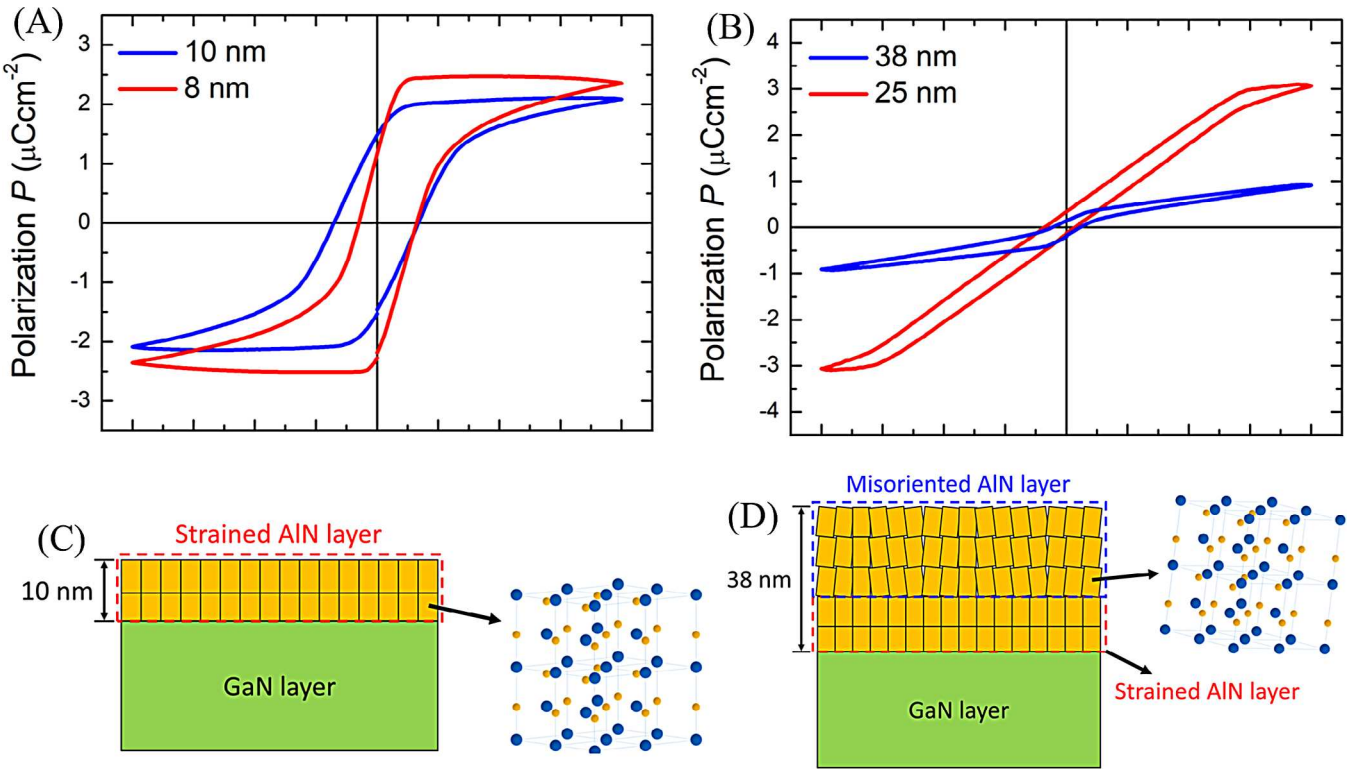

FIGURE 1 Polarization hysteresis loops for the AlN thin film with thickness of 8 and 10 nm (A), and 25 and 38 nm (B) measured at 2000 Hz, respectively. Schematic illustration of strain distribution difference between the 10-nm (C) and 38-nm (D) AlN thin films. Reprinted from Ref. 36 with the permission of SPIE Publications.

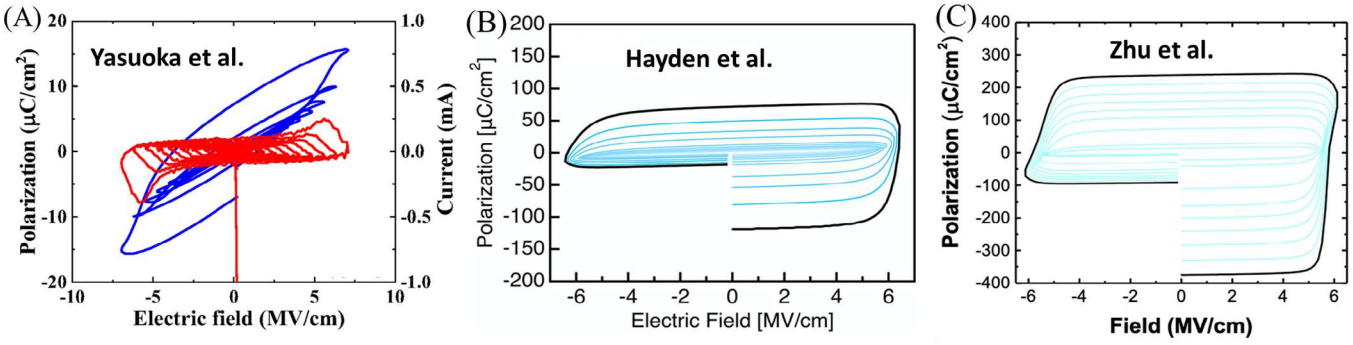

FIGURE 2 (A) Polarization hysteresis loops for a 140-nm AlN film measured at 100 kHz. (B) Polarization hysteresis loops for a 500-nm AlN film measured with a 200 Hz triangular wave. (C) Polarization hysteresis loops measured at 200 Hz for a 500-nm AlN film at 100°C. (A) Reprinted from Ref. 32 with the permission of AIP Publishing. (B) Reprinted from Ref. 26 with the permission of American Physical Society. (C) Reprinted from Ref. 38 with the permission of AIP Publishing.

breakdown strength as the authors have believed. As for P_r and E_c, both trend in the similar manner to that observed by Fichtner et al.[25] as shown in Figure 3C.

In addition, Wolff et al.[41] demonstrated the first atomic scale evidence for ferroelectric polarization inversion on the unit cell level in an epitaxial $Al_{0.75}Sc_{0.25}N$ thin film. The film was prepared by magnetron sputtering on a sapphire substrate at ~450°C with the final film thickness of 550 nm. The new formation of Al-polar inversion domains induced by electric field in the originally N-polar film is unambiguously determined by atomic resolution imaging using aberration-corrected scanning transmission electron microscopy (STEM), as shown in Figure 3D. Moreover, the STEM results are further substantiated by anisotropic etching showing a complete and homogenous polarization inversion at the film surface for the switched regions and

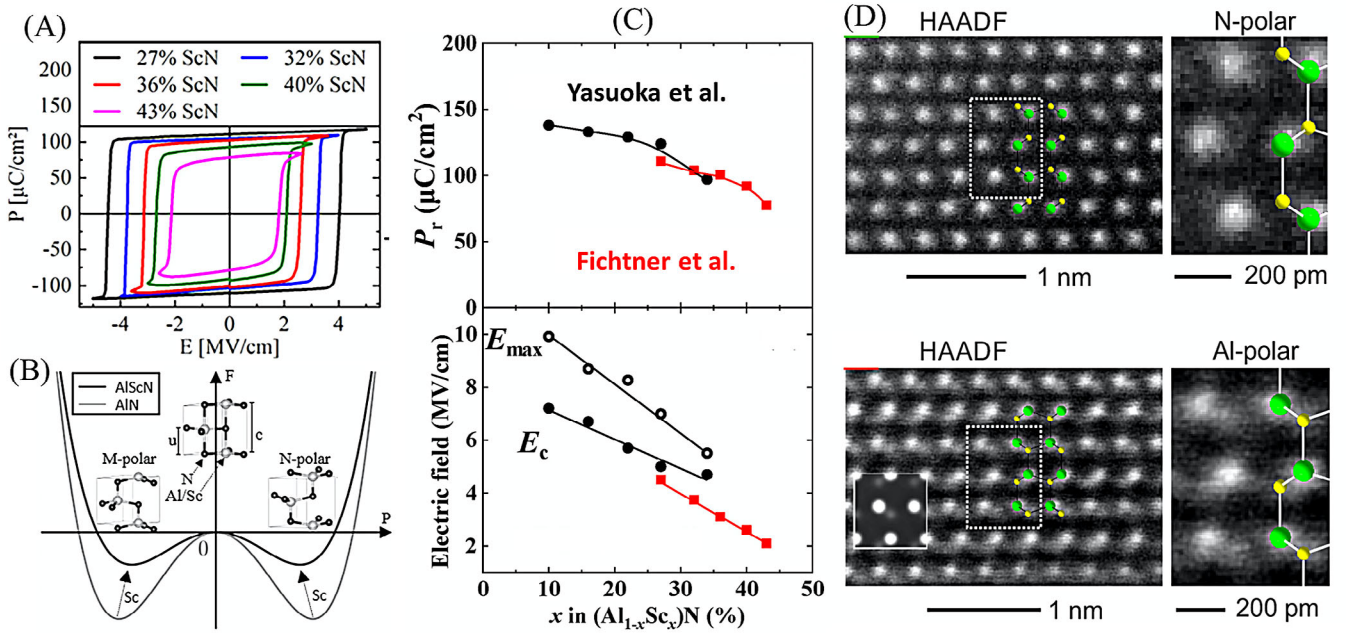

FIGURE 3 (A) Polarization hysteresis loops of ferroelectric $Al_{1-x}Sc_xN$ thin films with $x = 0.27, 0.32, 0.36, 0.40, 0.43$. (B) Illustration of potential landscape flattening with addition of Sc to AlN. The two potential wells correspond to M-polar and N-polar wurtzite structure, and the intermediate transition state corresponds to a nonpolar layered hexagonal structure. (C) Sc composition dependence of P_r and E_c with data from Fichtner et al.[25] and Yasuoka et al.[32] (D) Demonstration of N-polar atomic structure in the as-deposited domain and Al-polar atomic structure in the switched domain by high angle annular dark field (HAADF) micrographs. (A) Reprinted from Ref. 25 with the permission of AIP Publishing. (B) Reprinted from Ref. 4 with the permission of AIP Publishing. (C) Reprinted from Ref. 32 with the permission of AIP Publishing. (D) Reprinted from Ref. 41 with the permission of AIP Publishing.

absence of previous inversion domain in the as-deposited regions.

3.2 | Effect of film deposition atmosphere and substrate

One critical aspect to achieve ferroelectric switching in $Al_{1-x}Sc_xN$ thin films is to ensure that E_c is lower than the dielectric breakdown field strength, which fortunately can be tuned by the film deposition process. For instance, Yasuoka et al.[32] investigated the effect of film deposition atmosphere on ferroelectricity of an $Al_{0.78}Sc_{0.22}N$ thin film. Specifically, the film was prepared by the dual-source reactive magnetron sputtering method from Al and Sc metal targets on a Si substrate, with the sputtering pressure maintained at 0.67 Pa by flowing in a mixture of N_2 and Ar gases (N_2:Ar = 2:1) or pure N_2 gas. As shown in Figure 4A, it is found that the film deposited with N_2 gas exhibits larger P_r than that with N_2/Ar mixture, suggesting considerable pinning of polarization for the latter. Structurally, it is identified that the out-of-plane lattice in *c*-axis increases, while the in-plane lattice in *a*-axis decreases for films deposited with N_2/Ar mixture. However, the exact mechanism of the structure change leading to partial polarization pinning has not been elucidated.

In addition, Yasuoka et al.[42] further investigated the deposition substrate effect on characteristics of ferroelectricity by depositing a 145-nm thick $Al_{0.8}Sc_{0.2}N$ film on various substrates with different thermal expansion coefficients (CTE) at 400°C. Specifically, four types of substrates, including fused silica, Si, Al_2O_3, and MgO, were used for the study, with CTE of 0.54, 4.0, 7.7, and 13.5×10^{-6}°C^{-1}, respectively. It is expected that the CTE mismatch between the substrates and $Al_{0.8}Sc_{0.2}N$ thin film would result in different amount of strain upon cooling from the deposition temperature. By theory and calculation, the $Al_{0.8}Sc_{0.2}N$ film would undergo in-plane tension for films deposited at fused silica and Si substrate, while undergo in-plane compression for films deposited at Al_2O_3 and MgO substrates. Figure 4B shows the polarization hysteresis loops for these films. Interestingly, E_c tends to increase with increasing substrate CTE, while P_r remains nearly constant. Figure 4C further shows the $2P_r$ value obtained by the positive-up-negative-down (PUND) measurement as a function of the applied electric field. Clearly, P_r for all the films tends to saturate well against the applied electric field and changes according to the substrate CTE.

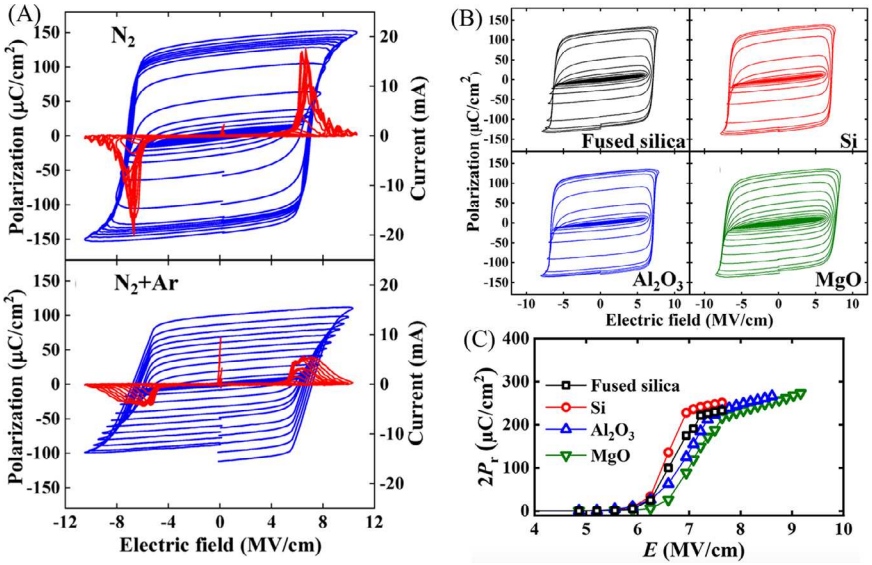

FIGURE 4 (A) Polarization hysteresis loops of ferroelectric $Al_{0.78}Sc_{0.22}N$ thin films deposited under pure N_2 and N_2/Ar mixture atmosphere with thickness of ~140 nm. (B) Polarization hysteresis loops of ferroelectric $Al_{0.8}Sc_{0.2}N$ films deposited on fused silica, Si, Al_2O_3, and MgO substrates with thickness of ~145 nm. (C) The corresponding $2P_r$ obtained by positive-up-negative-down (PUND) measurement as a function of applied electric filed. (A) Reprinted from Ref. 32 with the permission of AIP Publishing. (B and C) Reprinted from Ref. 42 with the permission of American Chemical Society.

The effect of deposition substrate can be theoretically explained by Yazawa et al.[31] in which they conducted a thermodynamic analysis of strain effect on ferroelectric $Al_{1-x}Sc_xN$ films using the classic Landau–Devonshire approach and showed that strain sensitivity of the energy barrier for ferroelectric switching in these wurtzite-type films is one order of magnitude larger than that of spontaneous polarization (P_r), which echoes well the large sensitivity of coercive field to strain/stress observed in many experiments.

3.3 | Thickness scaling of ferroelectricity

Thickness scaling in ferroelectric films can help reducing the size of ferroelectric devices, which is beneficial in reducing the power consumption. Conventional $Pb(ZrTi)O_3$ (PZT) films are known to lose ferroelectricity when the thickness goes below 100 nm,[43–45] while the ferroelectric HfO_2 film can go down to 3 nm while still maintain ferroelectricity.[17,18] As a novel ferroelectric material, understanding the thickness scaling of ferroelectricity in $Al_{1-x}Sc_xN$ films is critical.

Tasi et al.[33] prepared a series of $Al_{0.78}Sc_{0.22}N$ films by reactive sputtering at 400°C. The final film thickness varies from 10 to 47 nm. All the films are oriented along the *c*-axis as confirmed by X-ray diffraction (XRD). The ferroelectric-type hysteresis loops are observed in films with thickness as low as 20 nm. However, P_r shows a gradual degradation when the thickness is less than 35 nm by the PUND measurement. Similarly, Yasuoka et al.[32] prepared another series of $Al_{0.78}Sc_{0.22}N$ thin films with thickness varying from 9 to 139 nm. Their results show that the characteristic polarization hysteresis loop could be unambiguously observed for films with thickness of 48–139 nm. However, the ideal hysteresis loop disappeared when the film is thinner than 23 nm due to the large current leakage. Even though ferroelectricity is ascertained for films thinner than 23 nm from the PUND measurement, P_r is only 26 and 3.8 uC/cm^2 for the 23 and 9 nm thick film, respectively, which is much lower than the other films. Therefore, 20 nm seems to be the minimum thickness for $Al_{1-x}Sc_xN$ thin films to retain reasonable ferroelectric characteristics, which is substantiated by a recent study by Wang et al.[46] where a significant reduction of P_r is observed when the thickness is scaled down to below 20 nm for ferroelectric $Al_{0.7}Sc_{0.3}N$ thin films. Interestingly, results from Schönweger et al.[47] on $Al_{0.78}Sc_{0.22}N$ thin films, however, show moderate thickness scaling effect in the range of 10–100 nm, suggesting that the critical thickness for ferroelectricity is not yet approached down to 10 nm.

3.4 | Ferroelectric behavior at high temperature

The current ferroelectric devices based on perovskite or fluorite structure (e.g., $Pb(ZrTi)O_3$, (Hf, Zr, Si)O_2) cannot operate continuously at temperatures >200°C, which poses significant challenges to many critical high-temperature applications.[48,49] With the advent of $Al_{1-x}Sc_xN$ ferroelectric films, it is therefore crucial to understand their ferroelectric characteristics at high temperatures.

Drury et al.[34] systematically studied the temperature dependence of ferroelectric behavior for a 225-nm thick $Al_{0.7}Sc_{0.3}N$ thin film from ambient temperature to 400°C. Figure 5A shows the typical polarization hysteresis loops for the film at various temperatures. Interestingly, P_r undergoes insignificant changes, while E_c decreases

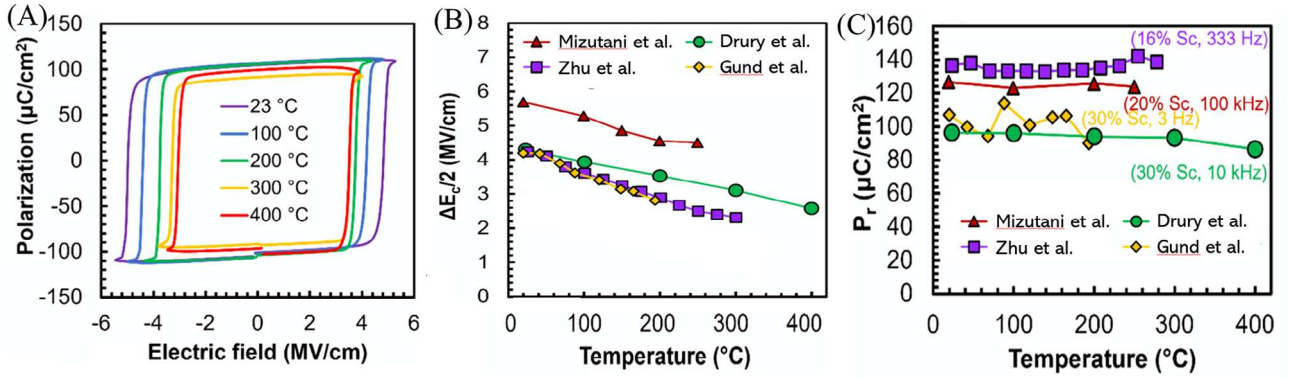

FIGURE 5 (A) Polarization hysteresis loops of a 225 nm thick $Al_{0.7}Sc_{0.3}N$ film measured with 10 kHz bipolar voltage waveform from 23°C to 400°C. Temperature dependence of E_c (B) and P_r (C) for various $Al_{1-x}Sc_xN$ thin films from various studies. Reprinted from Ref. 34 with the permission of MDPI.

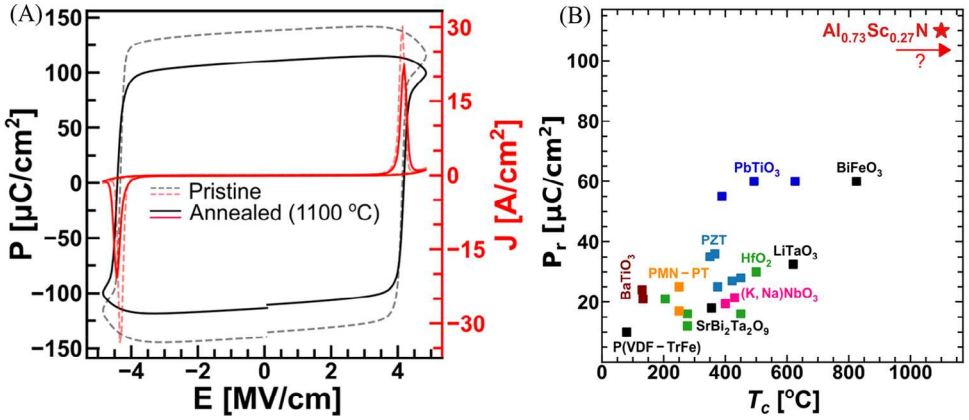

FIGURE 6 (A) Polarization hysteresis loops of *as-deposited* and *post-annealed* $Al_{0.73}Sc_{0.27}N$ thin films at 1100°C. Note that the corresponding switching current density curve is shown in red. (B) Comparison of P_r and lower limit of T_c of the $Al_{0.73}Sc_{0.27}N$ film with other known representative ferroelectric films: $BaTiO_3$,[53,54] PZT,[55] $BiFeO_3$,[56,57] $PbTiO_3$,[58] (K, Na)NbO_3,[59] HfO_2 based,[60–63] PMN-PT:$Pb(Mg_{0.33}Nb_{0.67})O_3$-$PbTiO_3$,[10,64] $LiTaO_3$,[65] and P(VDF-TrFe).[66] Reprinted from Ref. 35 with the permission of AIP Publishing.

dramatically from 4.3 to 2.6 MV/cm when temperature is ramped up to 400°C. The observation is consistent with multiple other studies[50–52] across different Sc contents and electric field frequency at shown in Figure 5B,C.

Islam et al.[35] further investigated the thermal stability of ferroelectric $Al_{1-x}Sc_xN$ thin films. They grew a series of $Al_{0.73}Sc_{0.27}N$ films with thickness ranging from 0.4 to 2 μm. The in situ structure and dielectric analysis show no sign of ferroelectric to paraelectric phase transition up to 1100°C. Moreover, ex situ scanning transmission electron microscopy analysis show that the structural change is insignificant, together with the moderate change of polarization hysteresis loop as shown in Figure 6A, it strongly indicates that conservation of the inscribed polarization state during the entire 1100°C annealing treatment. Therefore, the $Al_{1-x}Sc_xN$ thin films seem to have exceptional temperature stability compared to other alternative materials as shown in Figure 6B.

3.5 | Characteristics of endurance performance

The bandgap E_g of $Al_{1-x}Sc_xN$ films could be empirically expressed as $E_g(x) = -9.5x + 6.2$ (eV) for $0 < x < 0.34$, thus being insulators with a wide bandgap.[67] However, these ferroelectric films generally show unexpectedly large current leakage depending on deposition temperature and Sc content,[68–70] which poses significant challenges to the endurance and reliability performance in various device-level applications.

In an effort to illuminate the origin of current leakage, Kataoka et al.[71] conducted temperature-dependent current leakage analysis on a $TiN/Al_{0.78}Sc_{0.22}N/TiN$ capacitor fabricated by sputtering at Si substrate at 400°C with the final film thickness of 50 nm. It is found that the formation of nitrogen vacancies V_N at the metal interface lowers the Schottky barrier height ($\emptyset_{Bn}$) during the initial

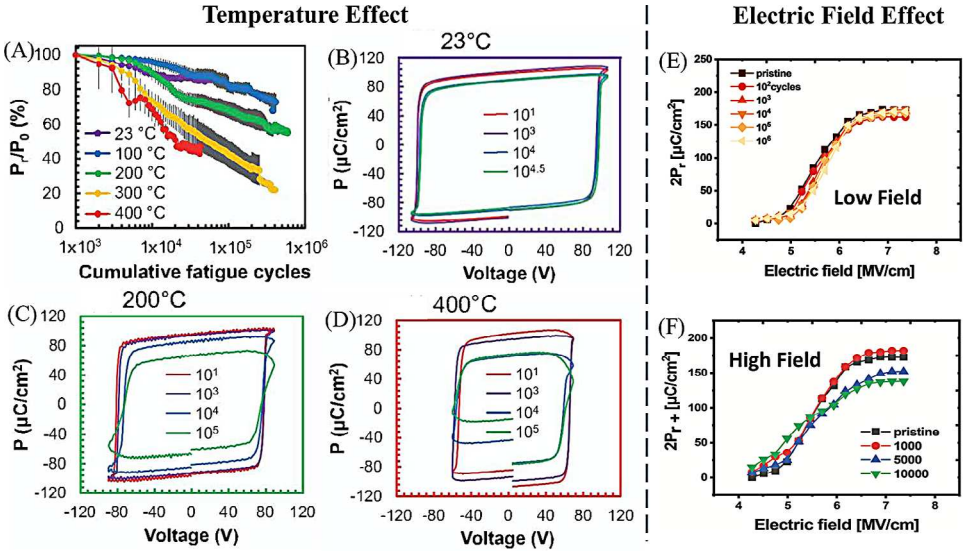

FIGURE 7 (A) Normalized P_r dependence of the $Pt/Al_{0.7}Sc_{0.3}N/Pt$ capacitor on fatigue cycles between 23°C and 400°C. The corresponding representative polarization hysteresis loops over the fatigue cycles at 23°C (B), 200°C (C), and 400°C (D). $2P_r$ of a $TiN/Al_{0.7}Sc_{0.3}N/TiN$ capacitor by positive-up-negative-down (PUND) measurement with different number of bipolar cycles for low electric field of 4.5 MV/cm (E) and high electric field of 7.5 MV/cm (F). (A–D) Reprinted from Ref. 34 with the permission of MDPI). (E and F) Reprinted from Ref. 73 with the permission of Wiley-VCH GmbH.

ferroelectric switching and leads to leakage current shift. Tsai et al.[72] from the same group further investigated the field cycling behavior and breakdown mechanism using the same capacitor setup. It is found that V_N emerges both in the bulk and at the near-interface region upon hundreds of switching cycles. The V_N creation in the bulk would facilitate the displacement of nitrogen atoms, creating ferroelectric domains with a low E_c. Upon further field cycling, electron trapping might occur in the bulk to pin the ferroelectric domains (especially for low E_c components) and reduce P_r to show fatigue behavior. In the near-interface region, continuous V_N creation would keep extending its territory to as deep as 6 nm with reduced $\emptyset_{Bn}$. Once the leakage current becomes sufficiently high, the capacitor breaks down due to the excessive heat generated.

In addition, Drury et al.[34] investigated the temperature dependence of fatigue behavior on a $Pt/Al_{0.7}Sc_{0.3}N/Pt$ capacitor fabricated using reactive magnetron sputtering on a Si substrate at 400°C with the final film thickness of 225 nm. The polarization hysteresis loop measurement was repeatedly conducted every 1000 cycles to track any polarization changes till to the breakdown point as shown in Figure 7A. Interestingly, the highest fatigue endurance occurs at 200°C with ~6.0×10^5 lifetime cycles. It could be explained by the fact that the reduction of E_c outpaces the breakdown point when temperature is ramped up to 200°C, thus resulting in an increasing margin between E_c and the breakdown point. However, once the temperature is over 200°C, the current leakage increases significantly, resulting in lower fatigue lifetime cycles.

Kim et al.[73] further investigated the effect of electric field strength on the fatigue behavior on a $TiN/Al_{0.7}Sc_{0.3}N/TiN$ capacitor fabricated by reactive magnetron sputtering with the final film thickness of 40 nm. The E_c for this film was around 6.5 MV/cm based on which both low electric field cycling (4.5 MV/cm) and high electric field cycling (7.5 MV/cm) were used for this study. Figure 7E,F shows the ferroelectric characteristics measured by the PUND method for low electric field cycling and high electric field cycling, respectively. Clearly, there is no noticeable change for P_r and fatigue occurrence in the low electric field cycling case. However, when the film is cycled with the high electric field, the $2P_r$ value decreases from ~175 to ~135 uC/cm^2 after 10 000 cycles, showing significant fatigue behavior. Therefore, the result appears to support the notion that polarization switching by high electric field facilitates V_N creation at the electrode/film interface resulting in an expansion of the non-ferroelectric interfacial dielectric layer upon continuous electric field cycling, and eventually leads to inducing charge trapping compromising polarization switching.

4 | FERROELECTRICITY IN $AL_{1-x}B_xN$ THIN FILM

A critical issue associated with ferroelectric $Al_{1-x}Sc_xN$ films is the undesired reduction of band gap from ~6.1 eV for $x = 0$ to as low as ~2.9 eV for $x = 0.45$, which contributes significantly to the current leakage at high Sc

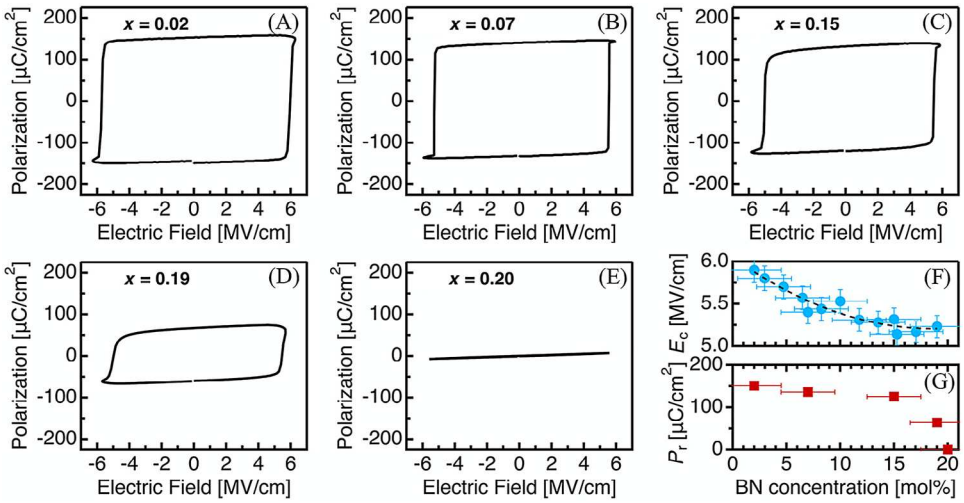

FIGURE 8 (A–E) Polarization hysteresis loops for a series of 500-nm thick $Al_{1-x}B_xN$ films with $x = 0$, 0.02, 0.07, 0.15, 0.19, 0.2 measured with a 200 Hz triangular wave. Dependence of E_c (F) and P_r (G) on boron concentration. Reprinted from Ref. 26 with the permission of American Physical Society.

content. In 2021, Hayden et al.[26] first reported ferroelectricity in boron-substituted AlN thin films with lower band gap reduction. The $Al_{1-x}B_xN$ films were grown by reactive magnetron sputtering on tungsten-coated Al_2O_3 substrate at 300°C with boron content ranging from 0 to 0.2. As clearly shown in Figure 8A–E, the films exhibit ferroelectric switching with P_r exceeding 125 uC/cm^2 for $0.02 \leq x \leq 0.15$ and retaining band gap over 5.2 eV. However, ferroelectricity gets significantly suppressed when $x > 0.15$, which might be associated with the steadily increasing crystallographic disorder with the noticeable *c*-axis orientation deterioration. Figure 8G,F further shows that E_c and P_r continuously trend down with increasing boron content, which is similar to that in the $Al_{1-x}Sc_xN$ ferroelectric system, but with less significant reduction.

Zhu et al.[38] furthered studied the temperature dependence of ferroelectric switching in $Al_{0.93}B_{0.07}N$ thin film, along with AlN and $Al_{0.84}Sc_{0.16}N$ films. The typical polarization hysteresis loops were measured for all the films from room temperature to 300°C as shown in Figure 9A,B. Both the $Al_{0.84}Sc_{0.16}N$ and $Al_{0.93}B_{0.07}N$ films show perfect box-like hysteresis loops with large P_r (~120–135 uC/cm^2) remaining nearly constant across the temperature range. However, E_c consistently decreases with increasing temperature for both films. Note that the pure AlN film only shows partial polarization switching in the study. The temperature dependence of E_c and P_r for these films are further clearly shown in Figure 9 C,D. Compared with the $Al_{0.84}Sc_{0.16}N$ film, the $Al_{0.93}B_{0.07}N$ film could maintain a higher E_c across the temperature range, which is consistent with the results from Hayden et al.[26]

In addition, Zhu et al.[74] studied the fatigue and retention behavior of a nearly 300-nm thick $Al_{0.93}B_{0.07}N$ film stacked between Pt/W and W electrode. It is found that the film is susceptible to dielectric breakdown upon bipolar cycling of 10^4–10^5 times, which initially leads to a leakage current increase and subsequently to localized failure events. The film also shows excellent retention of information storage with signal margins exceeding 200 uC/cm^2 after 1000 h baking at 200°C.

5 | SUMMARY AND OUTLOOK

To summarize, we carefully reviewed the latest developments on the ferroelectric characteristics of AlN-based thin films, including pure AlN, $Al_{1-x}Sc_xN$, and $Al_{1-x}B_xN$. Since ferroelectricity is only realized in these films over the past very few years, majority of the existing studies are focused on demonstrating ferroelectricity and examining ferroelectric characteristics phenomenologically with regard to film composition, temperature, film thickness, deposition condition, and fatigue endurance by electric field cycling. Among the relatively limited number of studies, $Al_{1-x}Sc_xN$ thin film has attracted most attention from a few research groups worldwide. With the latest discovery of ferroelectricity in $Al_{1-x}B_xN$ thin film in 2021, more research efforts are expected for this material due to its superior ferroelectric characteristics demonstrated so far. As for the pure AlN thin film, it is extremely challenging that unambiguous ferroelectricity can be achieved reliably in the near future.

Moving forward, we see an urgent need to combat the challenge of large current leakage faced by these novel AlN-based ferroelectric films. Identifying the root cause and coming up with engineering strategies to suppress the current leakage will be a critical step for industrial

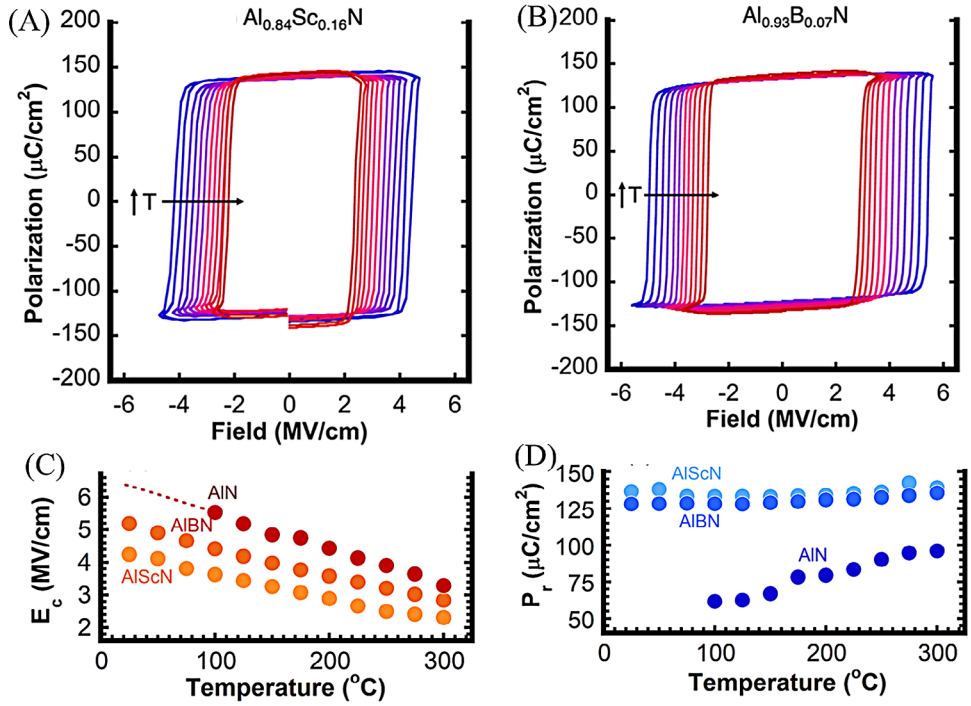

FIGURE 9 Polarization hysteresis loops for $Al_{0.84}Sc_{0.16}N$ (A) measured at 333 Hz and $Al_{0.93}B_{0.07}N$ (B) thin films at 100 Hz from room temperature to 300°C. The corresponding temperature dependence of E_c (C) and P_r (D) for these films. Note that the AlN film could not be fully saturated due to current leakage contributions. Reprinted from Ref. 38 with the permission of AIP Publishing.

applications. A combined efforts from both simulations and experiments are expected to play a significant role in tackling this problem. In addition, overcoming the thickness scaling challenge to push ferroelectricity down to a few nanometers for better device miniaturization will also be of great interest and importance. Lastly, inspired by the underlying working principle of ferroelectric realization in these AlN-based films, it may be also very rewarding to explore other III-V-based semiconductor materials for better ferroelectric characteristics.

ACKNOWLEDGMENTS

We thank the stimulating discussion with Prof. Jian Shi and Prof. Pawel Keblinski from Rensselaer Polytechnic Institute.

ORCID

Binghui Deng https://orcid.org/0000-0002-0460-4990
Yunfeng Shi https://orcid.org/0000-0003-1700-6049

REFERENCES

1. Mikolajick T, Schroeder U, Slesazeck S. The past, the present, and the future of ferroelectric memories. IEEE Trans Electron Devices. 2020;67(4):1434–43.
2. Martin LW, Rappe AM. Thin-film ferroelectric materials and their applications. Nat Rev Mater. 2017;2:16087.
3. Wan S, Peng Q, Wu Z, Zhou Y. Nonvolatile ferroelectric memory with lateral $\beta/\alpha/\beta$ In2Se3 heterojunctions. ACS Appl Mater Interfaces. 2022;14(22):25693–700.
4. Mikolajick T, Slesazeck S, Mulaosmanovic H, Park MH, Fichtner S, Lomenzo PD, et al. Next generation ferroelectric materials for semiconductor process integration and their applications. J Appl Phys. 2021;129(10):100901.
5. Megaw HD. Origin of ferroelectricity in barium titanate and other perovskite-type crystals. Acta Crystallogr. 1952;5(6):739–49.
6. Akbarian D, Yilmaz DE, Cao Y, Ganesh P, Dabo I, Munro J, et al. Understanding the influence of defects and surface chemistry on ferroelectric switching: a ReaxFF investigation of BaTiO3. Phys Chem Chem Phys PCCP [Internet]. 2019 [cited 2023 Apr 13];21(33). Available from: https://www.osti.gov/pages/biblio/1631259
7. Spanier JE, Kolpak AM, Urban JJ, Grinberg I, Ouyang L, Yun WS, et al. Ferroelectric phase transition in individual single-crystalline $BaTiO_3$ nanowires. Nano Lett. 2006;6(4):735–39.
8. Budd KD, Dey S, Payne DA. Sol-gel processing of $PbTiO_3$, $PbZrO_3$, PZT, and PLZT thin films. Br Ceram Proc. 1985;36:107–21.
9. Fu Z, Chen X, Li Z, Hu T, Zhang L, Lu P, et al. Unveiling the ferrielectric nature of $PbZrO_3$-based antiferroelectric materials. Nat Commun. 2020;11(1):3809.
10. Nishino R, Fujita TC, Kagawa F, Kawasaki M. Evolution of ferroelectricity in ultrathin $PbTiO_3$ films as revealed by electric double layer gating. Sci Rep. 2020;10(1):10864.

11. de Araujo CAP, Cuchiaro JD, McMillan LD, Scott MC, Scott JF. Fatigue-free ferroelectric capacitors with platinum electrodes. Nature. 1995;374(6523):627–29.
12. Amanuma K, Hase T, Miyasaka Y. Preparation and ferroelectric properties of $SrBi_2Ta_2O_9$ thin films. Appl Phys Lett. 1995;66(2):221–23.
13. Li AD, Ling HQ, Wu D, Yu T, Liu ZG, Ming NB. Characteristics of $SrBi_2Ta_2O_9$ ferroelectric films in an in situ applied low electric field prepared by metalorganic decomposition. Solid State Commun. 2003;125(9):469–73.
14. Wang J, Neaton JB, Zheng H, Nagarajan V, Ogale SB, Liu B, et al. Epitaxial $BiFeO_3$ multiferroic thin film heterostructures. Science. 2003;299(5613):1719–22.
15. Yun KY, Ricinschi D, Kanashima T, Noda M, Okuyama M. Giant ferroelectric polarization beyond 150 $\mu C/cm^2$ in $BiFeO_3$ thin film. Jpn J Appl Phys. 2004;43(5A):L647.
16. Botea M, Chirila C, Boni GA, Pasuk I, Trupina L, Pintilie I, et al. Lead-free $BiFeO_3$ thin film: ferroelectric and pyroelectric properties. Electron Mater. 2022;3(2):173–84.
17. Böscke TS, Müller J, Bräuhaus D, Schröder U, Böttger U. Ferroelectricity in hafnium oxide thin films. Appl Phys Lett. 2011;99(10):102903.
18. Tian X, Shibayama S, Nishimura T, Yajima T, Migita S, Toriumi A. Evolution of ferroelectric HfO_2 in ultrathin region down to 3 nm. Appl Phys Lett. 2018;112(10):102902.
19. Schroeder U, Yurchuk E, Müller J, Martin D, Schenk T, Polakowski P, et al. Impact of different dopants on the switching properties of ferroelectric hafniumoxide. Jpn J Appl Phys. 2014;53(8S1):08LE02.
20. Müller J, Böscke TS, Schröder U, Mueller S, Bräuhaus D, Böttger U, et al. Ferroelectricity in simple binary ZrO_2 and HfO_2. Nano Lett. 2012;12(8):4318–23.
21. Schroeder U, Park MH, Mikolajick T, Hwang CS. The fundamentals and applications of ferroelectric HfO_2. Nat Rev Mater. 2022;7(8):653–69.
22. Polakowski P, Riedel S, Weinreich W, Rudolf M, Sundqvist J, Seidel K, et al. Ferroelectric deep trench capacitors based on Al:HfO_2 for 3D nonvolatile memory applications. In: 2014 IEEE 6th International Memory Workshop (IMW). IEEE, Taipei, Taiwan, 2014. p. 1–4.
23. Fujii S, Kamimuta Y, Ino T, Nakasaki Y, Takaishi R, Saitoh M. First demonstration and performance improvement of ferroelectric HfO_2-based resistive switch with low operation current and intrinsic diode property. In: 2016 IEEE Symposium on VLSI Technology IEEE, Honolulu, HI, USA, 2016. p. 1–2.
24. Okuno J, Kunihiro T, Konishi K, Maemura H, Shuto Y, Sugaya F, et al. SoC compatible 1T1C FeRAM memory array based on ferroelectric Hf0.5Zr0.5O2. In: 2020 IEEE Symposium on VLSI Technology. 2020. IEEE, Honolulu, HI, USA, p. 1–2.
25. Fichtner S, Wolff N, Lofink F, Kienle L, Wagner B. AlScN: a III-V semiconductor based ferroelectric. J Appl Phys. 2019;125(11):114103.
26. Hayden J, Hossain MD, Xiong Y, Ferri K, Zhu W, Imperatore MV, et al. Ferroelectricity in boron-substituted aluminum nitride thin films. Phys Rev Mater. 2021;5(4):044412.
27. Tasnádi F, Alling B, Höglund C, Wingqvist G, Birch J, Hultman L, et al. Origin of the anomalous piezoelectric response in wurtzite ScxAl1-xN alloys. Phys Rev Lett. 2010;104(13):137601.
28. Wu Y, Laleyan DA, Deng Z, Ahn C, Aiello AF, Pandey A, et al. Controlling defect formation of nanoscale AlN: toward efficient current conduction of ultrawide-bandgap semiconductors. Adv Electron Mater. 2020;6(9):2000337.
29. Wang P, Wang D, Vu NM, Chiang T, Heron JT, Mi Z. Fully epitaxial ferroelectric ScAlN grown by molecular beam epitaxy. Appl Phys Lett. 2021;118(22):223504.
30. Wang P, Wang D, Mondal S, Hu M, Liu J, Mi Z. Dawn of nitride ferroelectric semiconductors: from materials to devices. Semicond Sci Technol. 2023;38(4):043002.
31. Yazawa K, Zakutayev A, Brennecka GL. A Landau–Devonshire analysis of strain effects on ferroelectric Al1−xScxN. Appl Phys Lett. 2022;121(4):042902.
32. Yasuoka S, Shimizu T, Tateyama A, Uehara M, Yamada H, Akiyama M, et al. Effects of deposition conditions on the ferroelectric properties of (Al1−xScx)N thin films. J Appl Phys. 2020;128(11):114103.
33. Tsai SL, Hoshii T, Wakabayashi H, Tsutsui K, Chung TK, Chang EY, et al. On the thickness scaling of ferroelectricity in Al0.78Sc0.22N films. Jpn J Appl Phys. 2021;60(SB):SBBA05.
34. Drury D, Yazawa K, Zakutayev A, Hanrahan B, Brennecka G. High-temperature ferroelectric behavior of Al0.7Sc0.3N. Micromachines. 2022;13(6):887.
35. MdR Islam, Wolff N, Yassine M, Schönweger G, Christian B, Kohlstedt H, et al. On the exceptional temperature stability of ferroelectric Al1-Xscxn thin films. Appl Phys Lett. 2021;118(23):232905.
36. Lin BT, Lee WH, Shieh J, Chen MJ. Ferroelectric AlN ultrathin films prepared by atomic layer epitaxy. Proceedings Volume 10968, Behavior and Mechanics of Multifunctional Materials XIII. 2019.
37. Dreyer CE, Janotti A, Van de Walle CG, Vanderbilt D. Correct implementation of polarization constants in wurtzite materials and impact on III-nitrides. Phys Rev X. 2016;6(2):021038.
38. Zhu W, Hayden J, He F, Yang JI, Tipsawat P, Hossain MD, et al. Strongly temperature dependent ferroelectric switching in AlN, Al1-xScxN, and Al1-xBxN thin films. Appl Phys Lett. 2021;119(6):062901.
39. Zhang S, Holec D, Fu WY, Humphreys CJ, Moram MA. Tunable optoelectronic and ferroelectric properties in Sc-based III-nitrides. J Appl Phys. 2013;114(13):133510.
40. Yazawa K, Mangum JS, Gorai P, Brennecka GL, Zakutayev A. Local chemical origin of ferroelectric behavior in wurtzite nitrides. J Mater Chem C. 2022;10(46):17557–66.
41. Wolff N, Fichtner S, Haas B, Islam MR, Niekiel F, Kessel M, et al. Atomic scale confirmation of ferroelectric polarization inversion in wurtzite-type AlScN. J Appl Phys. 2021;129(3):034103.
42. Yasuoka S, Mizutani R, Ota R, Shiraishi T, Shimizu T, Uehara M, et al. Tunable ferroelectric properties in wurtzite (Al0.8Sc0.2)N via crystal anisotropy. ACS Appl Electron Mater. 2022;4(11):5165–70.
43. Kim K, Lee S. Integration of lead zirconium titanate thin films for high density ferroelectric random access memory. J Appl Phys. 2006;100(5):051604.
44. Chu F, Fox G, Davenport T. High endurance scaled PLZT thin films for FRAM applications. Integr Ferroelectr. 2001;36(1–4):43–52.
45. Ihlefeld JF, Harris DT, Keech R, Jones JL, Maria JP, Trolier-McKinstry S. Scaling effects in perovskite ferroelectrics:

fundamental limits and process-structure-property relations. J Am Ceram Soc. 2016;99(8):2537–57.
46. Wang D, Wang P, Mondal S, Hu M, Wang D, Wu Y, et al. Thickness scaling down to 5 nm of ferroelectric ScAlN on CMOS compatible molybdenum grown by molecular beam epitaxy. Appl Phys Lett. 2023;122(5):052101.
47. Schönweger G, Islam MR, Wolff N, Petraru A, Kienle L, Kohlstedt H, et al. Ultrathin Al1−x Sc x N for low-voltage-driven ferroelectric-based devices. Phys Status Solidi RRL—Rapid Res Lett. 2023;17(1):2200312.
48. Stolichnov I, Tagantsev AK, Colla E, Setter N, Cross JS. Physical model of retention and temperature-dependent polarization reversal in ferroelectric films. J Appl Phys. 2005;98(8):084106.
49. Mueller S, Muller J, Schroeder U, Mikolajick T. Reliability characteristics of ferroelectric-thin films for memory applications. IEEE Trans Device Mater Reliab. 2013;13(1):93–97.
50. Wang J, Park M, Ansari A. High-temperature acoustic and electric characterization of ferroelectric $Al_{0.7}Sc_{0.3}N$ films. J Microelectromechanical Syst. 2022;31(2):234–40.
51. Mizutani R, Yasuoka S, Shiraishi T, Shimizu T, Uehara M, Yamada H, et al. Thickness scaling of $(Al_{0.8}Sc_{0.2})N$ films with remanent polarization beyond 100 $\mu C\ cm^{-2}$ around 10 nm in thickness. Appl Phys Express. 2021;14(10):105501.
52. Gund V, Davaji B, Lee H, Asadi MJ, Casamento J, Xing HG, et al. Temperature-dependent lowering of coercive field in 300 nm sputtered ferroelectric $Al_{0.70}Sc_{0.30}N$. In: 2021 IEEE International Symposium on Applications of Ferroelectrics (ISAF). 2021. IEEE, Sydney, Australia, p. 1–3.
53. Wemple SH, Didomenico M, Camlibel I. Dielectric and optical properties of melt-grown $BaTiO_3$. J Phys Chem Solids. 1968;29(10):1797–803.
54. Wieder HH. Electrical behavior of barium titanatge single crystals at low temperatures. Phys Rev. 1955;99(4):1161–65.
55. Udayakumar KR, Schuele PJ, Chen J, Krupanidhi SB, Cross LE. Thickness-dependent electrical characteristics of lead zirconate titanate thin films. J Appl Phys. 1995;77(8):3981–86.
56. Catalan G, Scott JF. Physics and applications of bismuth ferrite. Adv Mater. 2009;21(24):2463–85.
57. Wang N, Luo X, Han L, Zhang Z, Zhang R, Olin H, et al. Structure, performance, and application of $BiFeO_3$ nanomaterials. Nano-Micro Lett. 2020;12(1):81.
58. Ma W, Zhong J, Jian W. Curie phase transition and critical size for ferroelectricity in strained ultrathin $PbTiO_3$ and $BaTiO_3$: a phenomenological study. Ferroelectrics. 2017;507(1):86–101.
59. Rafiq MA, Costa ME, Vilarinho PM. Pairing high piezoelectric coefficients, d33, with high Curie temperature (TC) in lead-free $(K,Na)NbO_3$. ACS Appl Mater Interfaces. 2016;8(49):33755–64.
60. Polakowski P, Müller J. Ferroelectricity in undoped hafnium oxide. Appl Phys Lett. 2015;106(23):232905.
61. Schroeder U, Mueller S, Mueller J, Yurchuk E, Martin D, Adelmann C, et al. Hafnium oxide based CMOS compatible ferroelectric materials. ECS J Solid State Sci Technol. 2013;2(4):N69.
62. Shimizu T, Katayama K, Kiguchi T, Akama A, Konno TJ, Sakata O, et al. The demonstration of significant ferroelectricity in epitaxial Y-doped HfO_2 film. Sci Rep. 2016;6(1):32931.
63. Zhou D, Müller J, Xu J, Knebel S, Bräuhaus D, Schröder U. Insights into electrical characteristics of silicon doped hafnium oxide ferroelectric thin films. Appl Phys Lett. 2012;100(8):082905.
64. Ho JC, Liu KS, Lin IN. Study of ferroelectricity in the PMN-PT system near the morphotropic phase boundary. J Mater Sci. 1993;28(16):4497–502.
65. Yang T, gai Liu Y, Zhang L, ling Hu M, Yang Q, hui Huang Z, et al. Powder synthesis and properties of $LiTaO_3$ ceramics. Adv Powder Technol. 2014;25(3):933–36.
66. Ducharme S, Fridkin VM, Bune AV, Palto SP, Blinov LM, Petukhova NN, et al. Intrinsic ferroelectric coercive field. Phys Rev Lett. 2000;84(1):175–78.
67. Deng R, Evans SR, Gall D. Bandgap in Al1−xScxN. Appl Phys Lett. 2013;102(11):112103.
68. Wang D, Zheng J, Musavigharavi P, Zhu W, Foucher AC, Trolier-McKinstry SE, et al. Ferroelectric switching in Sub-20 nm aluminum scandium nitride thin films. IEEE Electron Device Lett. 2020;41(12):1774–77.
69. Zukauskaite A, Wingqvist G, Palisaitis J, Jensen J, POÅ Persson, Matloub R, et al. Microstructure and dielectric properties of piezoelectric magnetron sputtered w-ScxAl1−xN thin films. J Appl Phys. 2012;111(9):093527.
70. Wang D, Zheng J, Tang Z, D'Agati M, Gharavi PSM, Liu X, et al. Ferroelectric C-axis textured aluminum scandium nitride thin films of 100 nm thickness. In: 2020 Joint Conference of the IEEE International Frequency Control Symposium and International Symposium on Applications of Ferroelectrics (IFCS-ISAF). IEEE, Keystone, CO, USA, 2020. p. 1–4.
71. Kataoka J, Tsai SL, Hoshii T, Wakabayashi H, Tsutsui K, Kakushima K. A possible origin of the large leakage current in ferroelectric Al1−xScxN films. Jpn J Appl Phys. 2021;60(3):030907.
72. Tsai SL, Hoshii T, Wakabayashi H, Tsutsui K, Chung TK, Chang EY, et al. Field cycling behavior and breakdown mechanism of ferroelectric $Al_{0.78}Sc_{0.22}N$ films. Jpn J Appl Phys. 2022;61(SJ):SJ1005.
73. Kim KD, Lee YB, Lee SH, Lee IS, Ryoo SK, Byun S, et al. Evolution of the ferroelectric properties of AlScN film by electrical cycling with an inhomogeneous field distribution. Adv Electron Mater. 2023;9(5):2201142.
74. Zhu W, He F, Hayden J, Tran Q, Yang JI, Tipsawat P, et al. Unique ferroelectric fatigue behavior and exceptional high temperature retention in $Al_{0.93}B_{0.07}N$ Films [Internet]. arXiv; 2022 [cited 2023 Apr 12]. Available from: http://arxiv.org/abs/2208.06486

How to cite this article: Deng B, Zhang Y, Shi Y. Examining the ferroelectric characteristics of aluminum nitride-based thin films. J Am Ceram Soc. 2024;107:1571–1581. https://doi.org/10.1111/jace.19540